Engineering and Technology Journal

Effect of Copper Foam Baffles on Thermal Hydraulic Performance for Staggered Arrangement in a Duct

Karrar Gh. Fadhala[*], **Ekhlas M. Fayyadh** , **Ali F. Mohammed**

Mechanical Engineering Dept., University of Technology-Iraq, Alsina'a street, 10066 Baghdad, Iraq.
*Corresponding author Email: karraralb1@gmail.com

HIGHLIGHTS

- Experimental study of the copper foam baffle on heat transfer and friction factor.
- Study the grade influence of pore density for copper foam baffles at fixed porosity on the flow and thermal behavior.
- The copper foam baffles were compared with solid copper baffles.

ARTICLE INFO

ABSTRACT

Metal foam is a novel material recently utilized in baffles as an alternative to solid baffles for reducing flow resistance. However, copper foam baffles have been suggested in this research to overcome this issue. So, the experimental tests were carried out in a manufactured square channel (250 mm x 250 mm) and heated uniformly at the bottom wall of the test section. Its walls are mounted copper foam baffles at a fixed porosity of 95%. Baffles were fixed alternatively on the top and bottom of the walls in staggered mode between two successive baffles (center to center) and were kept constant at 250 mm. The experimental work was done for different grades of the pore density of copper foam (10, 15, and 20 pores per inch (PPI)) with a window cut ratio of 25% and a constant heat flux of 4.4 kW/m^2. Reynolds number was varied from 3.8x10^4 to 5.4x10^4. The data for conventional copper solid baffles were used to compare the effect of foam metal baffles. The obtained results manifested that relative to the solid-copper baffles, the copper foam baffles have a greatly lower friction factor, whereas the friction factor for the solid baffles and copper foam baffles (10, 15, and 20) PPI is about (460), and (20, 29, and 38) times, respectively above the smooth surface. Moreover, the results of previous work predicted the present experimental work very well.

1. Introduction

One of the most common passive heat transfer augmentation techniques in single-phase internal flows is using channels with baffles. This passive heat transfer improvement technology has been applied to various industrial applications, including internal cooling systems for gas turbine blades, electronic cooling devices, thermal regenerators, and labyrinth seals for turbo-machines. Despite this wide range of applications, the presence of these baffles causes the flow to separate and reattach, thus creating regions of reverse flow and high shearing rates that affect thermal-hydraulic performance. However, some researchers investigated the effect of the appropriate geometric parameters of the baffles, such as baffle height (or window cut ratio), baffle spacing, and the relative arrangement of baffles that gives the best heat transfer performance for a given pumping power or flow rate. For example, [1] studied the effect of window cut ratio for solid baffles on the flow and heat transfer characteristic at turbulent flow. The experiments were carried out in a rectangular channel with baffles arranged as staggered with heating at a constant wall heat flux along the top and the bottom using air as the working fluid. The tests were performed at turbulent flow with different values of window cut ratio of 0.3, 0.5, and 0.7. The study's findings demonstrated that the local and average heat transfer and pressure loss increase when the window cut ratio decreases and the Reynolds number increases. However, the pressure loss increase was much higher than the increase in the heat transfer coefficient. The impact of distance between the baffles in the models of shell-and-tube heat exchangers on the heat transfer and pressure drop was investigated [2] experimentally. The experiments were performed at a range of Reynolds numbers with different values of the distance between the baffles. The results demonstrated that for a fixed value of the Reynolds number, the heat exchange coefficient and the pressure drop increased as the distance between the baffles was increased. The analytical and experimental study of the turbulent flow in a rectangular channel with baffled sheets was conducted by [3]. It was found that the greatest fluctuations in the pressure and velocity fields occur near the deflectors. The dynamic behavior of a turbulent airflow passing through a

rectangular channel with the presence of transverse baffles was examined by [4]. A comparative study was performed numerically among two different types of baffles, such as flat rectangular and trapezoidal, arranged in overlapping in a channel. Another study was conducted by [5], who performed a complete numerical investigation of the vortex generator design and its impact on the enhancement of heat transfer in behavior using plate baffles in turbulent flow conditions for different baffle pitches and different Reynolds numbers. It was found that in addition to baffling surfaces, the vortex shedding generated by the baffle on the upper wall might also promote heat transfer. Also, as the distance between the baffles decreased, the friction coefficient increased. Moreover, the impact of changing the distance between the baffles on the thermal performance of a shell tube heat exchanger was evaluated using a numerical and theoretical investigation [6]. Five distinct cases were used. Their findings displayed that, as compared to an equal baffle spacing pattern, varying the spacing between the baffles with a centered spacing pattern might be used to improve heat exchanger performance. Numerical analysis was done by [7] to determine the effects of three different baffle configurations (convex core/convex peripheral, convex peripheral/concave core, and convex peripheral/convex core) on the thermo-hydraulic performance in heat exchanger-type shell tube. The variable Reynolds numbers in the shell side, inlet cold fluid temperature, baffle spacing, and window cutting ratio was considered. It was found that the heat exchanger performance was improved by convex peripheral/concave core design.

However, utilizing the solid baffles improves heat transfer. Still, on the other side, it causes an increased pressure drop and a higher local thermal stress at the baffle's root, leading to worry. There is another passive method for enhancing the thermohydraulic performance in thermal systems represented by porous media and open metal foam [8]. As a result, the use of porous baffles to reduce pressure loss was studied by many researchers, such as [9], who performed an experimental study to investigate the effect of porous-type baffles on the heat transfer and friction in a baffles channel. Where the set of baffles was arranged staggered on the bottom and heated top walls of the channel. The porous-type baffled channel had less friction loss than the solid-type baffled channel. As a result, with a constant pumping power, the porous-type baffled channel produced higher thermal performance than the solid-type baffled channel. This experimental data was limited for this case and, therefore, as a preliminary to looking at a more realistic problem. Therefore, [10] extended the work of [9] numerically to study the effect of porosity porous baffles, window cut ratio, and Reynolds number on the flow and heat transfer characteristics. In addition, their results were compared with the experimental results [9]. It was found that the porous-type baffle channel has a lower friction factor than the solid-type baffle channel. Increasing the porous baffle heights has an insignificant effect on heat transfer augmentation. Furthermore, the effect of pore density for the porous baffle, window cut ratio, and baffle thickness on the friction factor and heat transfer was studied experimentally by [11] using aluminum foams baffles as heat sinks|. Their results elucidated that the staggered porous metal foam blocks with a pore density of 20 PPI can reduce the frictional resistance in the channel by three-quarters compared with the solid baffles having the same structure and size**.** Some researchers [12] carried out an experimental study of heat transfer and friction in duct with fully-perforated (open area ratio of 46.8%) or half-perforated baffles (open area ratio of 26%) for turbulent flow. The study depicted that the half-perforated baffles have better thermo-hydraulically performance than the fully-perforated baffles at the same pitch. The same research group [13] extended their work experimentally to investigate the effect of baffle pitch on the thermo-hydraulic performance of perforated baffles. They found that half-perforated baffles have a higher improvement in thermo-hydraulic performance than fully-perforated baffles. [14] studied experimentally the pressure drop and heat transfer in a channel with a low aspect ratio mounted in its staggered carbon foams working as porous baffles. As well as the effect of the channel blockage ratio on the heat transfer coefficient and pressure drop was included. It was observed that although the heat transfer was high both in a channel with solid baffles and in a channel with porous baffles; however, the porous baffles created a lower pressure drop. The impact height of the aluminum foam sample with a grade of 40 PPI and a porosity of 93% on the heat transfer and pressure drop were investigated experimentally by [15] using air as a working fluid. It was observed that the utilized metallic foam caused an increased thermal conductivity of the coolant and lower pressure losses than that of the solid baffles. Other investigators for the heat sink, such as [16], examined experimentally how the gap height of aluminum foam fins affects the fluid flow and heat transfer characteristics. It was observed that the Nusselt number is significantly impacted by the usage of higher gap heights. The same research group [15] extended their work experimentally [17] to investigate the impact channel blockage ratio for various grades of the aluminum foam blocks (5, 20, and 40) PPI at a fixed porosity of 93.8% on the heat transfer and pressure drop. The results showed that the aluminum foam blocks lead to better thermal performance with lower pressure drops than those generated with solid aluminum blocks. The effects of pore density of materials, channel blockage ratios, and inlet velocities on the flow characteristics of partially filled channels were experimentally studied by [18]. Their results showed that the pressure drop increased with the inlet velocity, pore density, and blockage ratio. However, the influence of using porous baffles on the thermo-hydraulic performance in a segmental baffle for the shell side flow of a shell tube heat exchanger was investigated numerically by [19] and compared it with heat exchangers with and without traditional baffles. It was found that the metal-foam baffles can reduce the pressure drop effectively. That is to say, adopting the metal-foam baffle can promote the comprehensive performance of heat exchangers effectively. [20] studied numerically the effect of the baffle cut for the porous baffles on the thermal-hydraulic performance. It was shown that the low baffle cuts produced the most heat transfer, but they also produced a substantial pressure reduction.

Surveying the overhead literature indicates that the large pressure drop of traditional baffles can be avoided by adopting porous baffles. Nevertheless, the authors found in the enhancement of heat transfer, limited experimental data exist relating to copper foam baffled-channel when considering the significant amount of research that has been conducted on the other types of porous baffles concerning thermal and flow behavior, in addition to the thermal-hydraulic performance of it. Therefore, the present work aims to study the influence of different grades of pore density (10, 15, and 20) PPI for open-copper foam baffles at a fixed porosity of (95%) on the flow and thermal behavior as well as the thermal-hydraulic performance. The experiments

have been carried out at a heated square duct with a constant heat flux of (4.4 kW/m^2) at turbulent flow within a range of Reynolds number from (3.8x10^4) to (5.4x10^4) using air as a working fluid.

2. Experimental Setup

The experimental setup, as presented in Figure 1, was divided into four major components: (1) air supply system; (2) test section; (3) test specimens, and; (4) measurement system. The flow system was suction-operated and horizontally orientated. Air is drawn into the channel entrance and flows through the test section downstream, and finally, it reaches the settling chamber linked to the air blower by a flexible air duct to minimize the vibration and noise. The flow rate was controlled using the sliding gate. The Perspex square channel has an internal size of 250 mm X 250 mm X 3125 mm, which consists of an entrance section, a test section, and an exit section of lengths 1125, 1000, and 1000 mm, respectively. A 10 mm-thick heated copper plate was used as the bottom wall of the test section. The copper plate was heated from the bottom by supplying uniform heat flux (4.4 kW/m^2) using a heating element, as revealed in Figure 1.
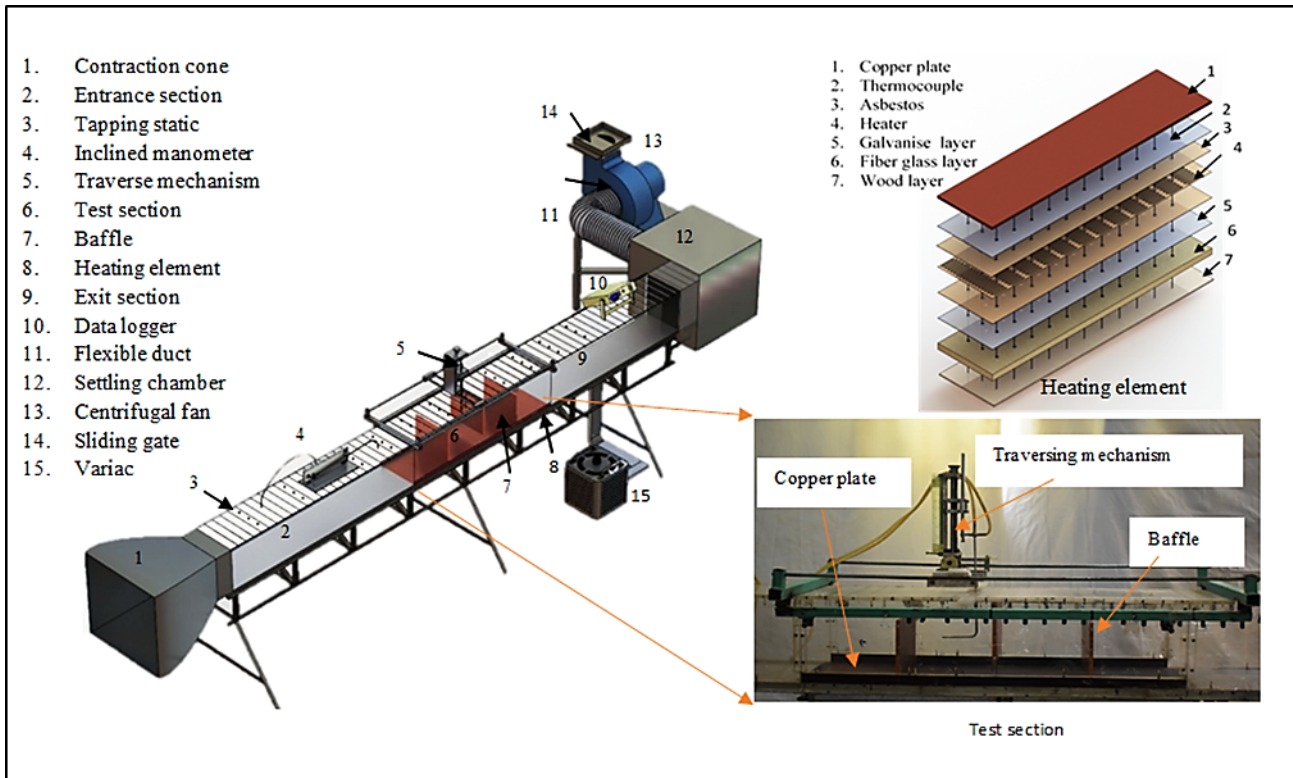

Figure 1: Experimental setup

The power supplied to the heating element is controlled by a variac and measured by a power meter Hameg HM8115-2 with an accuracy of ±0.4% for both current and voltage. Three baffles were fixed alternately at the test section and staggered into the top and bottom walls. Four models of copper baffles were used in this study, as displayed in Figure 2. Model 1 was solid baffles, and models 2, 3, and 4 were open cell types of uniform copper foam with different grades of pore density (10, 15, and 20) PPI and fixed porosity (95%). Table 1 lists the physical properties of copper baffles. These baffles have a depth of 250 mm, baffle spacing of 250 mm, baffle thickness of 10 mm, and window cut of 60 mm. Baffles were glued with the copper heated surface (bottom surface) of the test section by a thin layer of thermally conductive epoxy glue produced by Shenzhen Halnziye Electronics Company Ltd. While the other walls of baffles were glued with the side walls and top surface of the test section firmly using thermal epoxy. To measure the bottom wall temperature (the heated copper plate) for the test section by type K thermocouples, the heated copper plate was drilled from the backside with several holes (33) distributed in the x-y plane with equal distances at three rows and eleven columns. Therm compound paste was used to ensure proper contact between the thermocouples and the heated copper plate. A traverse thermocouple was used to measure the air-temperature distribution at the inlet and outlet of the test with K-type thermocouples. All thermocouples and data logger (Applent AT4532x) were calibrated with an accuracy of ±0.01 K. The temperature was recorded by the data logger (Applent AT4532x). The pressure drop across the test section for the different baffles configurations was measured with MK 4 & 5 Inclined Manometer type, which was connected to pressure taps fixed at 80 mm upstream and downstream of the test section with (1 Pa) accuracy. Pitot-static tube of 1 mm diameter was used to measure the magnitude of the velocity. The probe is provided with a traversing mechanism and MK 4 & 5 Inclined Manometer type with a precision of ±1. The differential pressure and temperatures under steady state were measured for each inlet velocity.
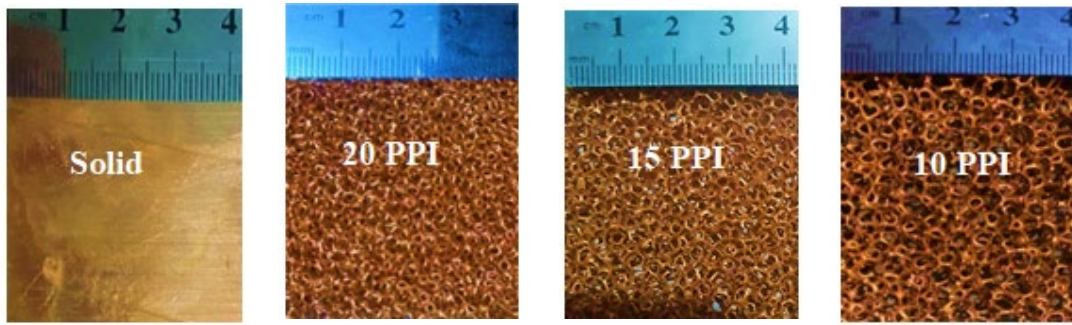
Figure 2: Models of copper baffles

Table 1: The physical properties of copper baffles

Model	PPI (-)	K (m²) E-07	E (%)	Metal (-)
Model 1	-	-	-	Solid copper
Model 2	10	2.61	0.95	Uniform copper foam
Model 3	15	2.18	0.95	Uniform copper foam
Model 4	20	1.56	0.95	Uniform copper foam

3. Data Reduction

The Reynolds number based on hydraulic diameter $D_h = 4A_c/2(W+H)$ was determined as follows [10]:

$$Re_{Dh} = \frac{u_b D_h}{v} \tag{1}$$

Where, u_b is the average velocity of air at the test section. The friction factor in a baffled channel flow can be determined by measuring the pressure drop ΔP across the test section and the average velocity of the air. Then, the friction factor was calculated from the Equation below [11]:

$$f = \frac{[(\Delta P/l)D_h]}{\rho_a u_b{}^2/2} \tag{2}$$

Where, l denotes the length of the test section. The bulk temperature (T_b) of air was calculated from Equation [1]

$$T_b = \int_0^H |u|T dy / \int_0^H |u| dy \tag{3}$$

Then, the bulk temperature of the air at any arbitrary point inside the test section was calculated using the mass flow rate and the net heat flow at the same point. The net heat input to the heated element Q_i of the baffled test section is defined as [1]:

$$Q_i = \dot{m}C_p (T_{bo} - T_{bin})_i \tag{4}$$

Where T_{bo} and T_{bin} is the bulk temperature of the air at the outlet and inlet of the heated element at the baffled test section, respectively, and $\dot{m}$ is the mass flow rate of air that passes through the test section, which is defined as:

$$\dot{m} = \rho_a \, Ac \, u_b \tag{5}$$

The heat flux $q_i^{''}$ was calculated as follows [1]:

$$q_i^{''} = \frac{Q_i}{Wx_i} \tag{6}$$

Where W and x_i denote the width and length of the heated element at the bottom wall of the test section, respectively. The local heat transfer coefficient h_{li} through the test section was then evaluated from the following Equation [1]:

$$h_{li} = \frac{q_i^{''}}{(T_{wi} - T_{bi})} \tag{7}$$

Where, T_{bi} is the bulk temperature of the air and T_{wi} is the wall temperature of heating element. The average convective heat transfer coefficient was calculated as follows [1]:

$$\bar{h} = \frac{1}{l}\int_0^l h_{li} dx \tag{8}$$

246

Then, the average Nusselt number was calculated as follows [1]:

$$\overline{Nu} = \frac{\bar{h}D_h}{k_f} \qquad (9)$$

In all calculations, the values of the thermo-physical properties of air were obtained at the bulk mean temperature. The performance evaluation criterion (η) was used to compare the enhanced forms of an original configuration, and plain configuration [21], which was determined as the ratio of the Nusselt number to the friction factor raised to the power of 1/3 as described by the Equation below [11]:

$$\eta = \left(\frac{[\overline{Nu}/(f)^{1/3}]_{baffle}}{[\overline{Nu}/(f)^{1/3}]_{smooth}} \right) \qquad (10)$$

The heat losses were less than 15%. Experimental data were acquired at atmospheric pressure over the following ranges of parameters: Reynolds number $Re_{Dh} = (5.4 \times 10^4 - 3.8 \times 10^4)$ and heat flux $q'' = 4.4$ kW/m^2. Steady-state values of the heating wall and air temperatures in the duct at various locations were used to determine the heat transfer coefficient, average Nusselt number, friction factor and thermal performance parameter values. The propagated uncertainty analysis was conducted using the method explained in [22], and the values were 7.5% and 21.1% for friction factor and average Nusselt number, respectively.

4. Results and Discussion

4.1 Validation of The Experimental Data

To validate the experimental procedure and start the current study with the baffles, the results of friction factors and average Nusselt numbers for the smooth channel without baffles in the present work for a fully developed flow are compared to those provided in the literature. So, the variation of friction factor with Reynolds number for fully developed flow in straight channels is shown in Figure (3A). This figure shows the experimentally measured friction factor compared with the correlation of Kays and Perkins (1985) [23] for a fully developed flow. The comparison shows that the experimental results gave the same trend as the experimental results of Kays and Prekins (1985), with a difference of about 59%. Also, the experimental average Nusselt number was compared with the correlation of Dittus–Boelter [24], as shown in Figure (3B). It is noticed from the figure that the experimental values appear to have a similar trend with the correlation, where the average Nusselt number increased with increasing Reynolds number, with a deviation between them of about (22%). This divergence is most likely the result of the different cross-sectional areas employed in the present study versus the circular section used in the Dittus-Boelter correlation.
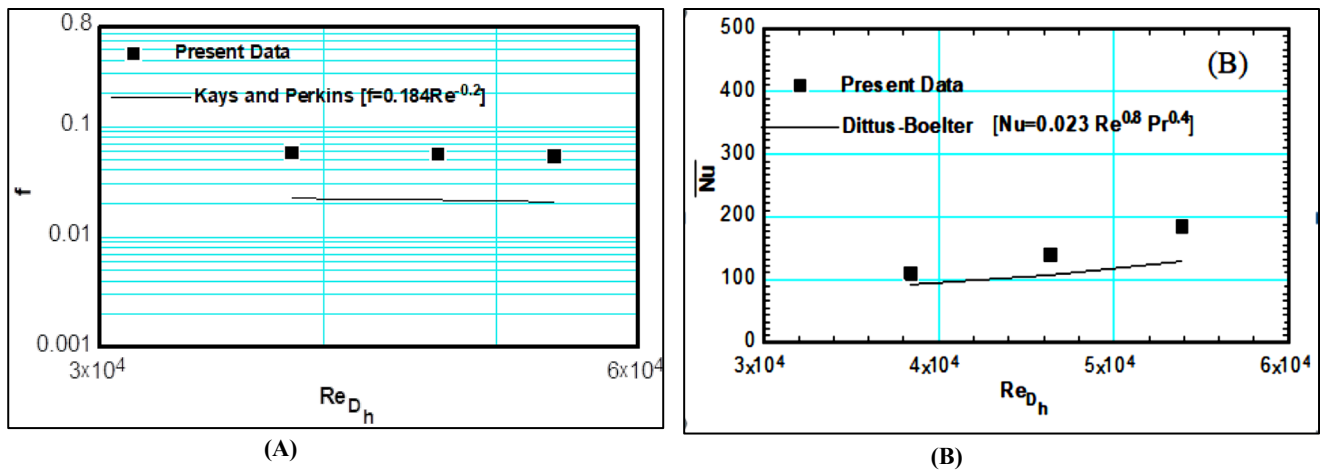

Figure 3: Comparison of present experimental work with previous work at a smooth surface for (A) Friction factor and (B) Average Nusselt number

4.1 Velocity Distribution for The Baffled Channel

4.1.1 Effect of Reynolds number on velocity distribution for the solid baffled- channel

The influence of solid baffle on the velocity distribution before the first baffle, after the third baffle, and between the baffles is depicted in Figure 4. As shown in this figure, at a low Reynolds number (3.8×10^4), at a distance of x = 1.397 m from the entry, and corresponds to a dimensionless axial position of x/L=0.43, the dimensionless axial velocity (u/U_{max}) decreased when the flow is approaching the lower part of the first baffle. While in the space between the top of the baffle and the top wall of the channel, the flow accelerates and approaches 40% of the maximum velocity, which is 3.5 m/s.

Considering the figure, it will be observed that the negative values of the dimensionless axial velocity between the first and the second baffle at a distance equal to 0.15 m beyond the first baffle, located at position x = 1.647 m from the inlet of the tunnel corresponding to the dimensionless axial location of x/L=0.507. The negative value of the dimensionless axial velocity is a function of the flow separation (recirculation zone), which is located close to the solid baffle and the bottom surface of the channel. Also, high velocities have been observed in the region between the summit of the baffle and the upper wall of the channel, nearest to the value of 200% of the maximum velocity, that is (10.5 m/s). This increasing velocity between the baffle's sharp edges and the channel wall surfaces was due to the higher dynamic pressure values caused by the reduction in the passage of the flow stream. As expected, the current flow is detached on the front top edge of the second solid baffle, leading to negative axial velocities on the rear region of this same second baffle as shown in Figure 4 at a dimensionless axial location of x/L = 0.58 m (i.e., location x = 1.885 m from the entrance of the channel with 0.15 m after the second baffle). The negative velocities refer to a recirculation zone with very strong cells for recycling. Contrarily, the flow velocity is increasing in the lower half of the channel, especially towards the passage under the second baffle, approaching 314% of the maximum velocity, which is 14.5 m/s. However, the region of negative values observed at the dimensionless axial location of x/L = 0.507 will decay at a dimensionless axial location of x/L = 0.67. Here, the velocity profile is almost invalid in the lower part of the channel. In comparison, in the higher part, the air accelerates again towards the gap of the last solid baffle and at the channel exit section. Passing the final section (x/L= 0.67), the value of axial velocity is higher than the maximum velocity, approaching 424%, which is 18.34 m/s; this was agreed with [3]. These values are generated due to the high recirculation flow in the rear of the second baffle. According to the figure, as the Reynolds number increased from 3.8×10^4 to 5.4×104, the dimensionless axial flow velocity tended to increase at all locations, and the size of the recirculation zones increased.
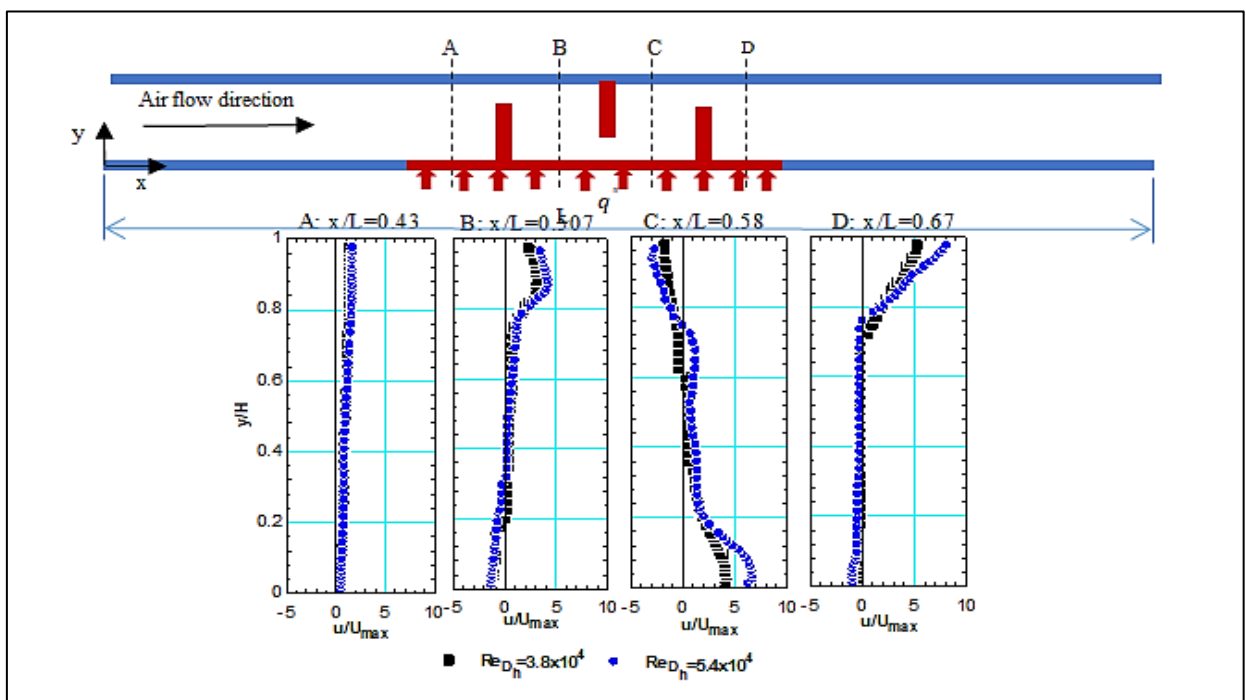

Figure 4: Velocity distribution across the test section of solid baffles at different locations streamwise direction for different Re_{Dh} of (3.8×10^4 and 5.4×10^4)

4.1.2 Effect of Reynolds number on velocity distribution for the metal foam baffled channel

The effects of Reynolds number within a range of 3.8×10^4 and 5.4×10^4 on the velocity profile for copper foam baffles having a pore density of 20 PPI are displayed in Figure 5. At a given Reynolds number value, it is clear that the velocity profile for the porous-type baffles is entirely different from solid baffles (as shown in Figure 4 due to various transport phenomena. The recirculation zone (i.e., negative velocity) found the backward of the solid copper baffle vanishes in the same region as that of the copper foam baffle. When the flow passes across the copper foam baffles, a part of the coming flow tends to pass into the copper foam baffles that, directly affect the recirculation region, leading to decay. Here, the magnitude of the velocity is lower than the maximum velocity. This emphasizes that the air entering pores begins to lose momentum due to colliding ligaments and continues to flow through pores along the path to the backward of the copper foam baffles. The remainder of the flow passes through the gap between the summit of the baffles and the channel wall; here, the flow accelerates. Considering the figure, when one compares the velocities at the dimensionless axial locations (x/L) of (0.43, 0.507, 0.58, and 0.67) within the range of Reynolds number 3.8×10^4 - 5.4×10^4, it is noticed that the maximum dimensionless axial velocity for these locations is approaching to 1.14, 1.71, 1.612, and 1.646 respectively at $Re_{Dh}=3.8 \times 10^4$ and 1.144, 1.933, 1.798 and 1.948 at $Re_{Dh}=5.4 \times 10^4$.
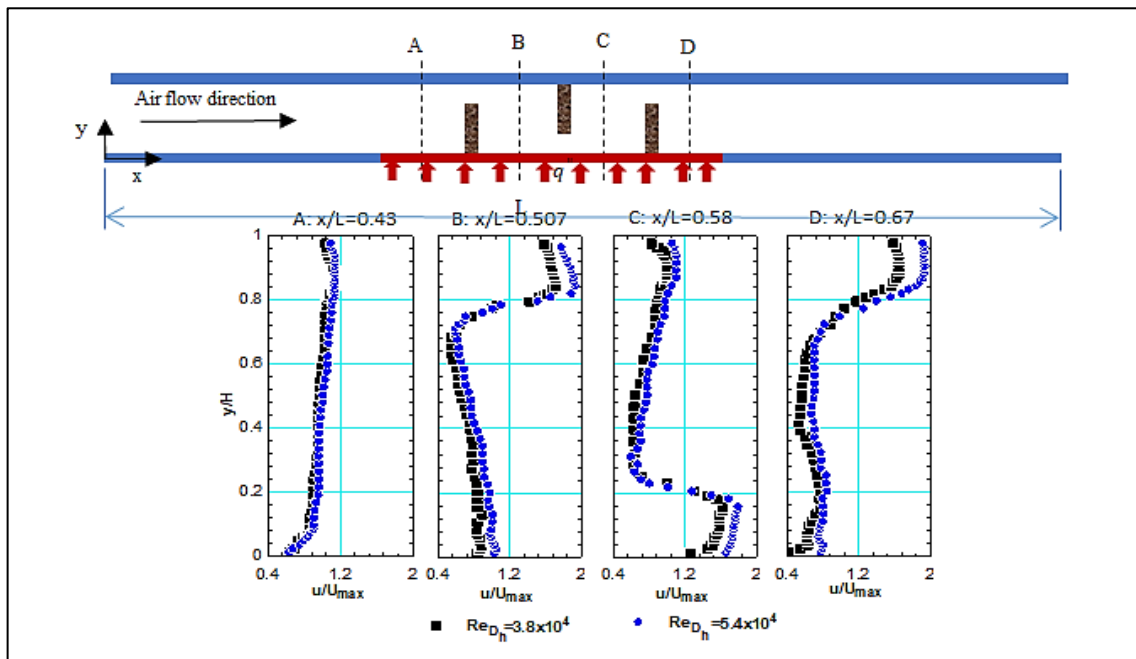
Figure 5: Velocity distribution across the test section of copper foam baffles with 20 PPI and fixed porosity (95%) at different locations of streamwise direction for different Re_{Dh} values (3.8 x10^4 and 5.4 x10^4)

4.1.3 Effect of pore density on velocity distribution for the copper foam baffled channel

The impact of increasing pore density from 10 up to 20 PPI on the dimensionless axial velocity across the copper foam-type baffles with constant porosity (0.95) is manifested in Figure 6 at dimensionless axial locations (x/L) for 0.43, 0.507, 0.58, and 0.67 with a similar Reynolds number (5.4x10^4). It is clear from this figure that for copper foam baffles with a pore density of 20 PPI, the airflow passes through the gap between the edge of the baffles and the channel wall with the maximum dimensionless axial velocity, compared to the copper foam baffles with a pore density of 15 and 10 PPI. This drives home the point that the baffles made of copper foam with smaller pores (20 PPI) have a higher resistance to flow; hence, the air is more inclined to keep away from the foam having higher pore density.

When one compares the maximum dimensionless axial velocities at the dimensionless axial locations of 0.43, 0.507, 0.58, and 0.67 for copper foam baffles, it is noticed that it is approaching 38.5%, 63.6%, 79.8%, and 60% of the maximum velocity, respectively for pore density 10 PPI and 34.7%, 58.7%, 76.1%, and 56.5% of the maximum velocity, respectively for pore density 15 PPI, while 31.5%, 54.5%, 73.3%, and 47.5% of the maximum velocity, respectively for pore density 20 PPI. So, depending upon the concept of mass conservation, only a small amount of the airflow has passed through the copper foam with a pore density of 20 PPI. While the copper foam with a lower pore density of 10 PPI has higher flow rates passing through it.
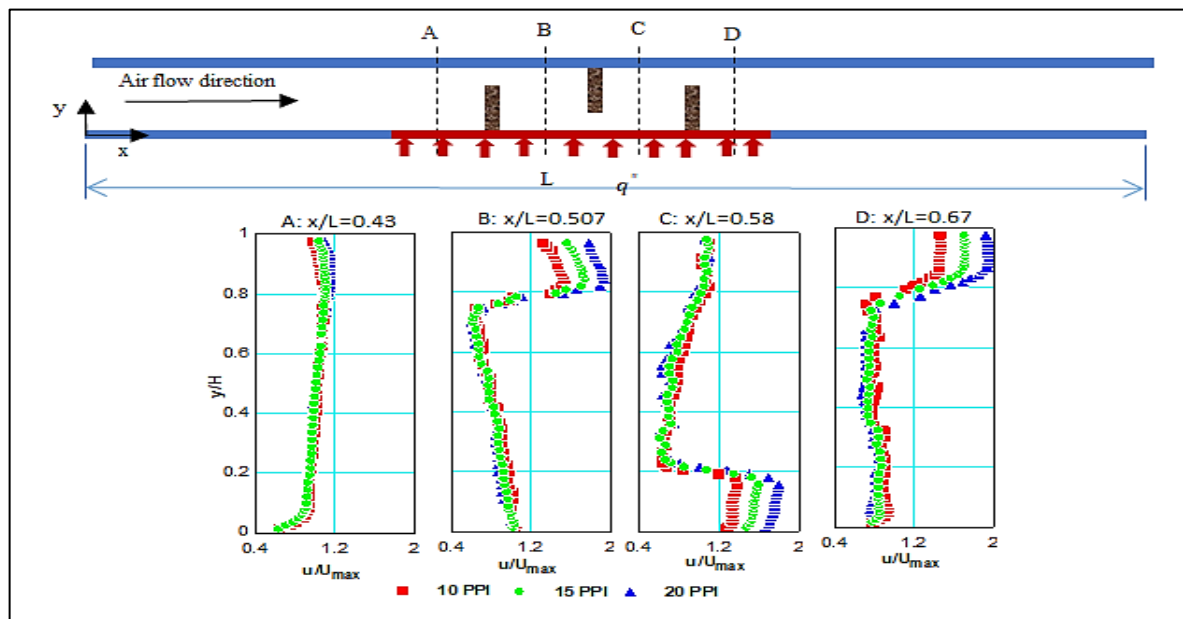

Figure 6: Velocity distribution across the test section of copper foam baffles with different grades of pore density, and fixed porosity (95%) at different locations of streamwise direction for a Re_{Dh} of (5.4 x10^4)

5. Temperature Distribution for The Baffled Channel

5.1.1 Effect of Reynolds number on temperature distribution for the solid baffled channel

The influence of increasing Reynolds number from 3.8×10^4 to 5.4×10^4 on the temperature distribution through the channel with the baffles at four dimensionless axial locations (0.43, 0.507, 0.58, and 0.67) is elucidated in Figure 7. Generally, for a given Reynolds number, the temperature increases along the test section from upstream to downstream of the baffles while passing through it. This is due to, as mentioned by [9] that as the flow crosses the solid copper baffle, the fluid that turns on from the bottom wall of the channel upstream of the baffle into the contraction area between the tip of the baffle and the channel wall creates a vigorous shear layer from the baffle summit to the bottom wall of the channel and that shapes a sizeable recirculation bubble backward of the baffle. The bending shear layer acts as an isolated wall that the heat transfer by convection prevents the recirculation zone from the main flow. As a result, this region has been associated with higher temperature distributions. As well as, it was noted from the figure a decrease in temperature in the area located between the gap of each baffle and the channel walls due to the lowering thermal conductivity of air.

However, it was observed that the temperature distribution is high at the downstream zone of the third baffle. This is related to alteration in the direction of the flow created by the baffle, where the highest temperature value demonstrates the backward of the lower wall of the channel with the acceleration process that starts shortly after the third baffle. According to the figure, one can see that as Reynolds number is increased from 3.8×10^4 to 5.4×10^4, the temperatures decrease slightly. In other words, a reverse proportionality was found between the increasing Reynolds number and the total temperature in the channel cross-section. Hence, the findings confirm that the low Reynolds numbers increase the thermal transfer between the air and the walls in the present investigation. Moreover, according to the analysis of dimensionless axial velocity and the temperature distribution for the all-dimensionless axial location inspected, it is concluded that the air temperature is linked to the flow velocity.
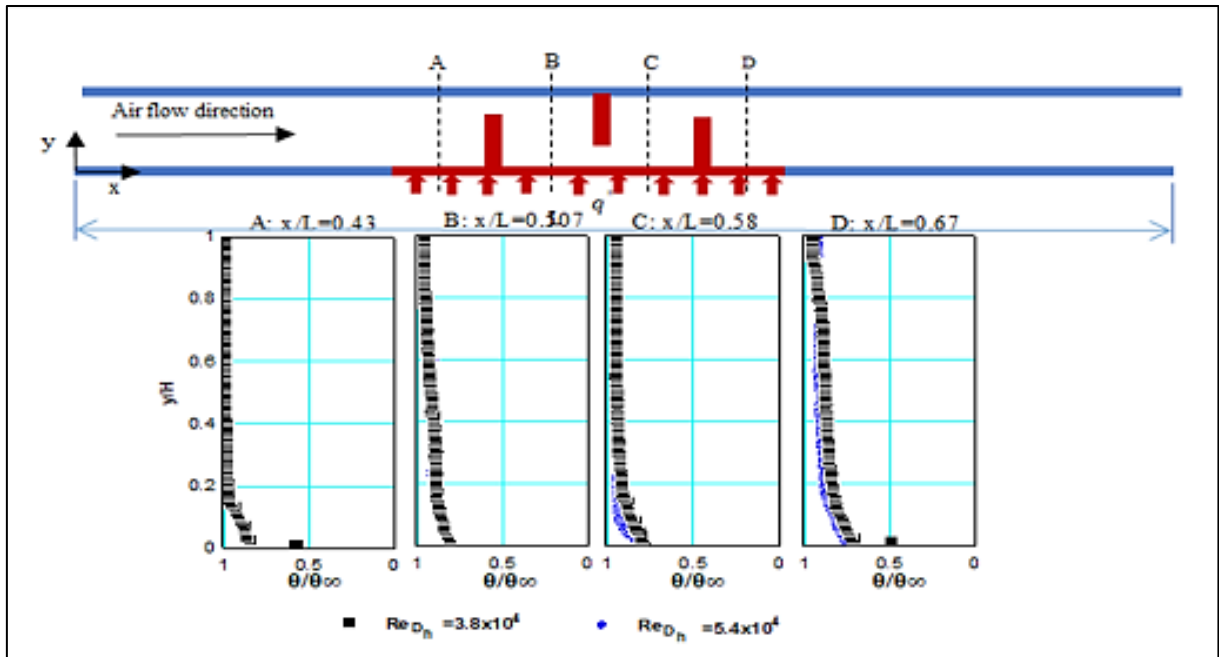

Figure 7: Temperature distribution across the test section of solid baffles at different locations streamwise direction for different Re_{Dh} values of (3.8 x104 and 5.4 x104)

5.1.2 Effect of Reynolds number on temperature distribution for the copper foam baffled channel

The influence of copper foam baffles with a pore density of 15 PPI and a fixed porosity of 95% on the temperature distribution from upstream baffles to downstream baffles, as well as between them, is displayed in Figure 8 at different dimensionless axial locations (0.43, 0.507, 0.58, and 0.67). In addition to the impact of increasing, the Reynolds number is revealed in the figure. Generally, for a given Reynolds number, it was found that the temperature distribution from the upstream to downstream of copper foam baffles is similar to the solid baffles but has a lower gradient of temperature distribution. As mentioned before, as the flow over copper foam baffles, a portion of the flow flows through the baffle's pore, lowering or eliminating the hot region and forming drag. This can be explained, as reported by [12], that as the flow passes through the pore of metal foam, it flows as a jet at the exit of it, which interacts with the reattaching and accelerates the flow across the baffles. Then, the reattachment effect is a bit reduced, but the flow through the pore generates turbulence at the wall of the channel that causes a decrease in the thickness of the viscous sublayer and mixing of the air close to the wall with the turbulent core.
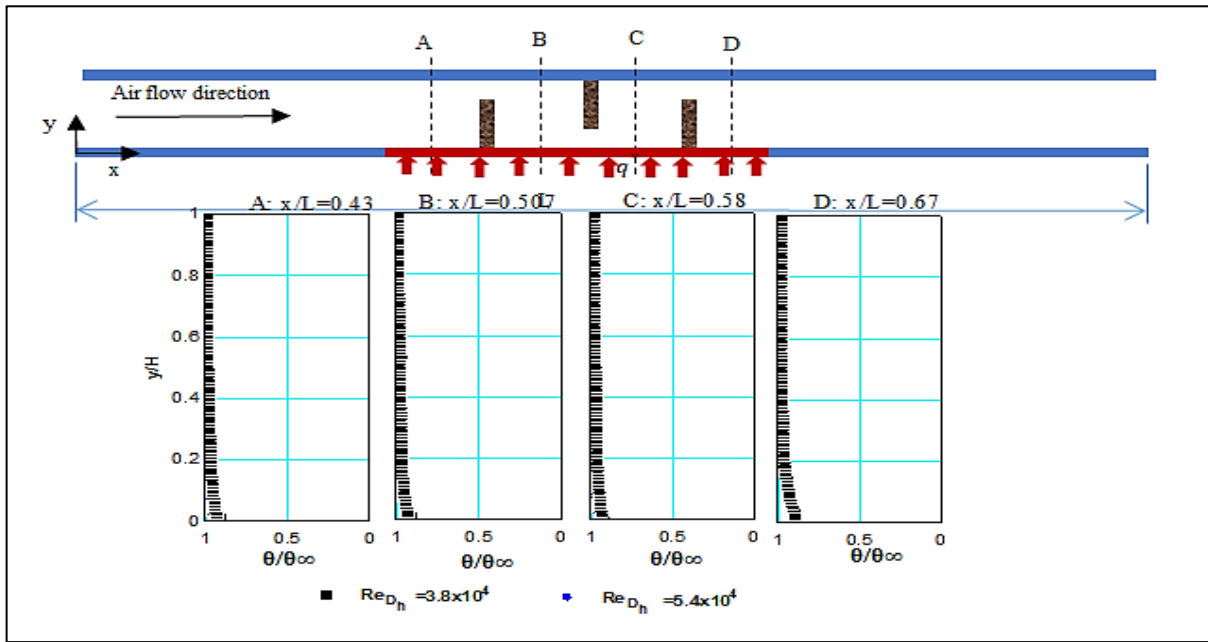
Figure 8: Temperature distribution across the test section of copper foam baffles with 15 PPI and fixed porosity (95%) at different locations of streamwise direction for different Re_{Dh} values of (3.8 x10^4 and 5.4 x10^4)

5.1.3 Effect of pore density

The impact of increasing pore density from 10 PPI up to 20 PPI of copper foam baffles with constant porosity (95%) on the temperature distribution is portrayed in Figure 9 at a dimensionless axial location (x/L) of (0.58) and a Reynolds number of (Re_{Dh}=5.4×10^4). It is clear from the figure that the air temperature gradient behind the copper foam baffles has a low value with pore density (10 PPI), and then it increased with increasing pore density of copper foam up to 20 PPI. As mentioned earlier, there is a difference between the flow flows through and on the top of copper foam baffles when the copper foam baffles have different pore densities, where the highest flow rate is with copper foam baffles with a pore density of 10 PPI compared with 20 PPI. It is known that conduction and convection are the principal heat transfer mechanism in foam baffles since the permeability (K) of copper foam with low pore density (10 PPI) is 2.61 x10^{-7} m^2, which is slightly higher than that of copper foam having a high pore density (20 PPI) of K=1.56x10^{-7} m^2. Therefore, the contribution of convection heat transfer from the total heat transfer for a copper foam baffle with low pore density is slightly higher than that of copper foam baffles with a pore density of 20 PPI. As a result, the convection heat transfer through the baffles with low pore density (10 PPI) was insufficient to increase the temperature of flowing air flow markedly.
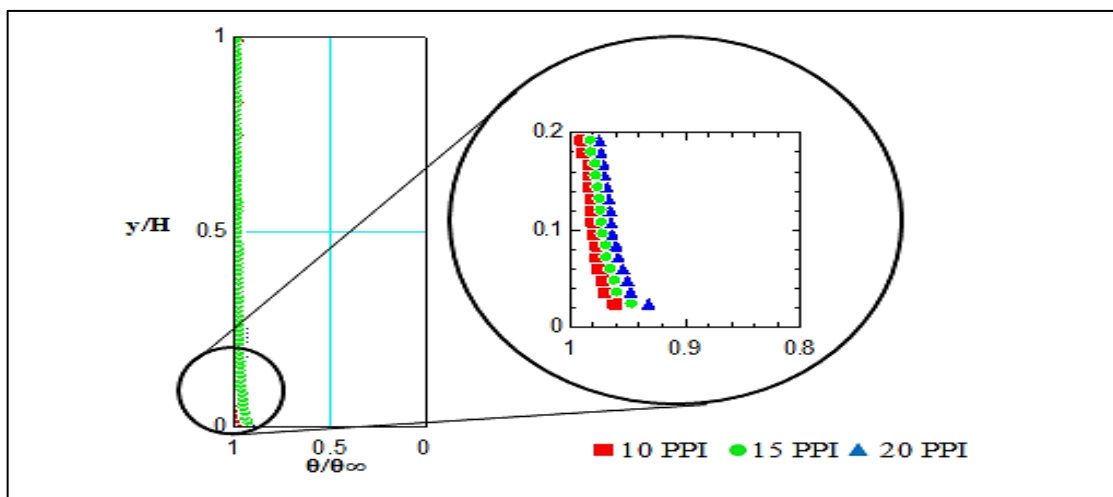

Figure 9: Effect of the grade pore density of copper foam baffles on the temperature distribution at axial location x/L=0.58 and fixed porosity 95% at a Re_{Dh} of 5.4×10^4

5.2 Friction Factor

The friction factor of the channel with and without baffles (solid and copper foam) as a function of the Reynolds number is illustrated in Figure (10 A). This figure exhibits that the friction factor for all baffles samples yields greater values with a similar trend compared to the smooth surface. Also, according to the figure, the friction factor for solid baffles is higher among

all specimens; using the baffles can motivate the recirculation to occur and appear backward from the baffles, as mentioned before, which cannot be observed on the smooth surface. The friction factor for the solid baffles and copper foam baffles (10, 15, and 20) PPI is about (450), and (20, 29, and 38) times, respectively, above the smooth surface. It can be concluded that the copper foam baffles have a much lower friction factor than the solid baffles. Also, it can be seen that the foam baffle with smaller pore sizes (20 PPI) generated a higher friction factor than baffles with larger pore sizes (15 and 10) PPI with an average of (30% and 45.9%). This behavior can be explained, as reported by [11], where increasing the pore densities lead to a higher specific surface area, resulting in a higher impedance of air from passing through it, i.e., a higher fraction of the stiff form impeding airflow. Also, the permeability is related to a pressure drop, where the higher permeability has a lower pressure drop and vice-versa. Hence, the permeability of copper foam with a pore density of 10 PPI is 2.61×10^{-7} m^2, while for copper foam with a pore density of 20 PPI, it is 1.56×10^{-7} m^2

6. Heat Transfer

The influence of the Reynolds number on the average Nusselt number for all types of baffles (solid and copper foam) is shown in Figure (10B). Also, the average Nusselt number for the smooth surface is presented in this figure for comparison. It can notice that the average Nusselt number for a channel with baffles (solid copper and copper foam (10,15, and 20) PPI) is higher than that of smooth surface with 407 %, 58%, 63%, 89%, respectively, for a given Reynolds number. So, the average Nusselt number of solid baffles has a higher value due to the flow mixing induced by the vorticity from the main flow, which breaks the thermal boundary layer as reported by [11]. Also, one can find that the augmentation of the average Nusselt number for the copper foam baffle having a higher pore density (20 PPI) is greater than that of copper foam baffles with a lower pore density (15 PPI and 10 PPI). This may be because an increase in pore density increases the contact surface area between the fluid and the solid, increasing the heat transfer enhancement.
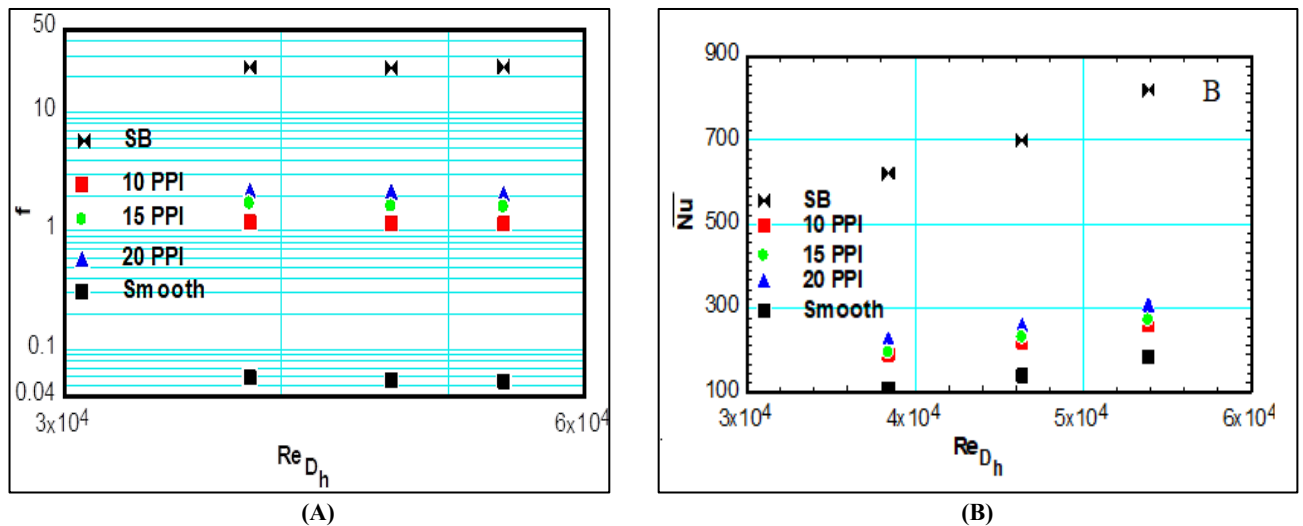

| (A) | (B) |

Figure 10: Comparison of present experimental work with previous work at a baffles case for (A) Friction factor and (B) Average Nusselt number

6.1 Thermo-Hydraulic Performance

The thermo-hydraulic performance (η) criterion provides an efficient way to evaluate the enhancement in thermo-hydraulic performance. This was used for trading off between the enhanced forms of an original configuration (i.e., a channel with baffles (solid/copper foam)) and a plain configuration (channel without baffles), which was determined as the ratio of the average Nusselt number to the friction factor raised to the power of 1/3. Hence, the thermal-hydraulic performance of all types of baffles in the channel is depicted in Figure 11. It is clear from this figure that the thermo-hydraulic performance was less than one. This agrees with [11], which explained that there are many applications where the pumping power is not inconsiderable, as in the case of a car or offshore drilling applications. So, the space may be outstanding in many situations, making the usage of lightweight foam baffles particularly appealing. According to the figure, the thermo-hydraulic performance decreases with an increase in Reynolds number. This is related to the fact that the turbulent effects dominate over the improvement at higher Reynolds numbers.

The enhancement of heat transfer relative to the friction factor with the presence of the baffles in the channel depends on the configuration of the baffles. Thus, by comparing the specimens of baffles as shown in Figure 11, one can find that the solid baffles are higher than the specimens of copper foam baffles (10, 15, and 20) PPI with 14%, 21.5%, and 16.6%. Also, it is clear from the figure that the thermo-hydraulic performance of the copper foam baffles with a pore density of 10 PPI is (8%) times and (3%) times higher than that of the copper foam baffles with a pore density of 15 and 20 PPI, respectively. This indicates that the excess pressure drop created by the copper foam baffles having a pore density of 15 and 20 PPI is more pronounced than the heat transfer enhancement.
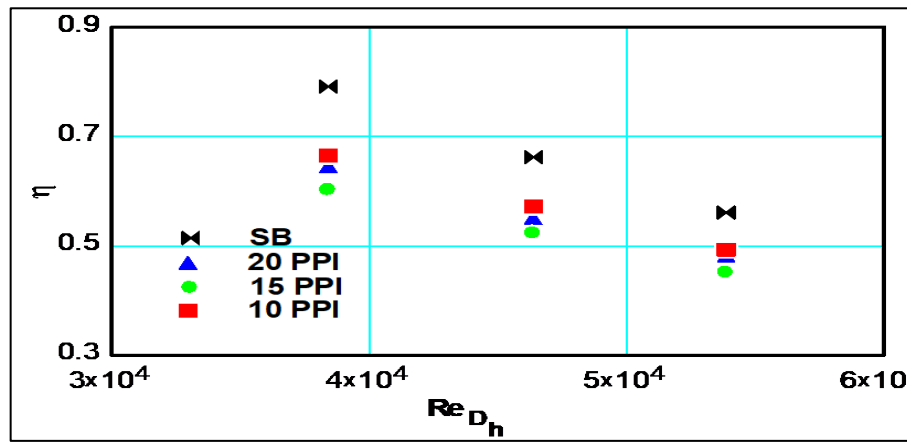
Figure 11: Variation of thermo-hydraulic performance with Reynolds number for various types of baffles

6.2 Comparison of The Present Experimental Work With Previous Work

The present experimental work was carried out for the three baffles that were mounted in a channel in a staggered manner with a window cut ratio of 25%, a pitch ratio equal to 0.96, and a constant heat flux of (4.4) kW/m^2 at the lower wall of the test section. The experimental data for $\overline{Nu_B}/\overline{Nu_s}$ and the thermo-hydraulic performance (η) of the current work for solid baffles and copper foam baffles with different grades of pore density 10 and 20 PPI was compared with the correlation presented by [11], as manifested in Figures (12 A) and Figure (12 B), respectively. The comparison for the $\overline{Nu_B}/\overline{Nu_s}$ and thermo-hydraulic performance indicates that the correlation predicted very well for the specimens of copper baffles with a solid plate and foam having a pore density of (10 and 20 PPI) with a mean absolute error (MAE) value of 10.1%, 8%, and 15.4%, respectively for the $\overline{Nu_B}/\overline{Nu_s}$ and with a MAE value of 17.1%, 16.5%, and 25.7% for the thermo-hydraulic performance.
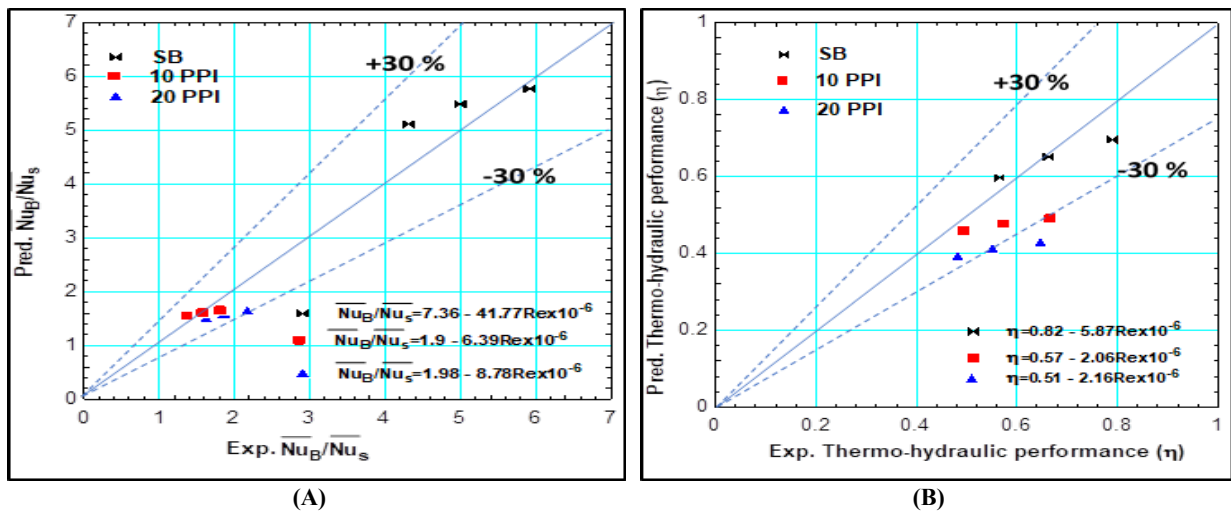

(A)

(B)

Figure 12: Comparison of the present experimental data with a correlation of [11]: (A) $\frac{\overline{Nu_B}}{\overline{Nu_s}}$ and (B) Thermo-hydraulic performance

7. Conclusion

Experiments were carried out for a turbulent flow in a square channel with a heated lower wall to study the effect of solid baffles and copper foam baffles with a fixed porosity of 95% on the flow and thermal behavior and the thermal-hydraulic performance. Baffles were mounted on the bottom, and top walls in a staggered fashion with a fixed spacing of (250 mm) and a window cut ratio of 25%. The results are presented for baffles with uniform copper foam (10, 15, and 20) PPI for the Reynolds number range (3.8×10^4-5.4×10^4). Also, the outcomes for solid baffles are manifested for comparison. The concluding remarks that can be drawn are as follows:

- Recirculation regions result from the low- and high-pressure regions at solid baffles. The most intense occurs downstream of the second solid baffle, responsible for higher axial flow velocities observed at (x/L= 0.67). The value of axial velocity was approaching 424% of the maximum velocity, which is 18.34 m/s.

- The transport phenomena across the baffles change when a copper foam baffle replaces a solid baffle in a channel, where the recirculation regions that were formed behind the solid baffles vanish in the identical region of the copper foam baffle.
- Relative to the solid-copper baffles, the copper foam baffles have a greatly lower friction factor, whereas the friction factor for the solid baffles and copper foam baffles (10,15, 20) PPI is about (450), and (20,29, and 38) times respectively above the smooth surface.
- The average Nusselt number for a channel having baffles (solid copper and copper foam (10,15, and 20) PPI) is significantly about 407 % and (58 %,63 %, and 89 %), respectively, higher than that of a smooth surface for a given Reynolds number.
- Thermal -hydraulic performance of the solid baffles is higher than specimens of copper foam baffles (10, 15, and 20) PPI with 14%, 21.5%, and 16.6%, respectively.

Nomenclature

A_c	Flow cross section area, m^2
C_p	Specific heat at constant pressure, J/kg.K
D_h	Hydraulic diameter, m
f	Friction factor
H	Channel height, m
h	Baffle height, m
h_l	Local heat transfer coefficient, $W/m^2.k$
$\bar{h}$	Average heat transfer coefficient, $W/m^2.k$
K	Permeability, m^2
k_f	Thermal conductivity, W/m.k
L	Length of tunnel, m
l	Length of test section, m
$\dot{m}$	Mass flow rate of air, kg/s
P	Pressure, Pa
Q	Heat convection, W
$q"$	Heat flux, kW/m^2
T	Bulk temperature, K
u	Local velocity, m/s
u_b	Average velocity of air, m/s
W	Channel width, m
X	Axial coordinate
Y	Vertical coordinate

Greek symbols

ε	Porosity
η	Thermo-hydraulic performance
ν	Kinematic viscosity, m^2/s
ρ	Density, kg/m^3
Δ	Difference

Subscripts

a	Air
b	Bulk, Baffles
i	Local
in	Inlet
o	Outlet
s	Smooth surface
w	Wall

Abbreviations

$\overline{Nu}$	Average Nusselt number
PPI	Pore per inch
Re_{Dh}	Reynolds number based on the channel hydraulic diameter

Acknowledgment

Author contribution

All authors contributed equally to this work.

Data availability statement

The data that support the findings of this study are available on request from the corresponding author.

Conflicts of interest

The authors declare that there is no conflict of interest.

References

[1] M.A. Habib, A.M. Mobarak, M.A. Sallak, E.A. Abdel Hadi, R.I. Affify, Experimental investigation of heat transfer and flow over baffles of different heights, J. Heat. Transfer., 116 (1994) 363–368. https://doi.org/10.1115/1.2911408

[2] H. Li, V. Kottke, Effect of baffle spacing on pressure drop and local heat transfer in shell-and-tube heat exchangers for staggered tube arrangement, Int. J. Heat. Mass. Transf., 41 (1998) 1303–1311. https://doi.org/10.1016/S0017-9310(97)00201-9

[3] L.C. Demartini, H.A. Vielmo, S. V. Möller, Numeric and experimental analysis of the turbulent flow through a channel with baffle plates, J. Brazilian Soc. Mech. Sci. Eng., 26 (2004) 153–159. https://doi.org/10.1590/S1678-58782004000200006

[4] H. Benzenine, R. Saim, S. Abboudi, O. Imine, Numerical simulation of the dynamic turbulent flow field through a channel provided with baffles: comparative study between two models of baffles: transverse plane and trapezoidal, Rev. Des Energies Renouvelables., 13 (2010) 639–651.

[5] R. Saim, H. Benzenine, H.F. Öztop, K. Al-Salem, Turbulent flow and heat transfer enhancement of forced convection over heated baffles in a channel, Int. J. Numer. Methods. Heat. Fluid. Flow., 23 (2013) 613–633. https://doi.org/10.1108/09615531311323773

[6] H. Bayram, G. Sevilgen, Numerical investigation of the effect of variable baffle spacing on the thermal performance of a shell and tube heat exchanger, Energies. 10 (2017). https://doi.org/10.3390/en10081156

[7] E.M.. El-Said, A.H. Elsheikh, H.R. El-Tahan, Effect of curved segmental baffle on a shell and tube heat exchanger thermohydraulic performance: Numerical investigation, Int. J. Therm. Sci., 165 (2021) 106922. https://doi.org/10.1016/j.ijthermalsci.2021.106922.

[8] N.M. Jasim, E.M. Fayyadh, M. Razoki Hasan, Numerical Analysis to Study the Effect of Foam Thickness on The Thermal-Hydraulic Performance of The Metal Foam Heat Exchanger, (2023) 357–373. https://doi.org/10.1007/978-981-19-1939-8_29

[9] J.J. Hwang, Turbulent heat transfer and fluid flow in a porous-baffled channel, J. Thermophys. Heat. Transf., 11 (1997) 429–436. https://doi.org/10.2514/2.6258

[10] Y.T. Yang, C.Z. Hwang, Calculation of turbulent flow and heat transfer in a porous-baffled channel, Int. J. Heat. Mass. Transf., 46 (2003) 771–780. https://doi.org/10.1016/S0017-9310(02)00360-5

[11] K.H. Ko, N.K. Anand, Use of porous baffles to enhance heat transfer in a rectangular channel, Int. J. Heat. Mass. Transf., 46 (2003) 4191–4199. https://doi.org/10.1016/S0017-9310(03)00251-5

[12] R. Karwa, B.K. Maheshwari, N. Karwa, Experimental study of heat transfer enhancement in an asymmetrically heated rectangular duct with perforated baffles, Int. Commun. Heat Mass Transf. 32 (2005) 275–284. https://doi.org/10.1016/j.icheatmasstransfer.2004.10.002

[13] R. Karwa, B.K. Maheshwari, Heat transfer and friction in an asymmetrically heated rectangular duct with half and fully perforated baffles at different pitches, Int. Commun. Heat. Mass. Transf., 36 (2009) 264–268. https://doi.org/10.1016/j.icheatmasstransfer.2008.11.005

[14] S. Mahadevan, M. Ricklick, J.S. Kapat, Internal Cooling Using Porous Turbulators: Heat Transfer and Pressure Drop Measurements, J. Thermophys. Heat. Transf., 27 (2013) 526–533. https://doi.org/10.2514/1.T3919

[15] A. Hamadouche, R. Nebbali, H. Benahmed, A. Kouidri, A. Bousri, Experimental investigation of convective heat transfer in an open-cell aluminum foams, Exp. Therm. Fluid. Sci., 71 (2016) 86–94. https://doi.org/10.1016/j.expthermflusci.2015.10.009

[16] K. Bilen, S. Gok, A.B. Olcay, I. Solmus, Investigation of the effect of aluminum porous fins on heat transfer, Energy. 138 (2017) 1187–1198. https://doi.org/10.1016/j.energy.2017.08.015

[17] A. Hamadouche, A. Azzi, S. Abboudi, R. Nebbali, Enhancement of heat exchanger thermal hydraulic performance using aluminum foam, Exp. Therm. Fluid. Sci., 92 (2018) 1–12. https://doi.org/10.1016/j.expthermflusci.2017.10.035

[18] F. Shikh Anuar, I. Ashtiani Abdi, M. Odabaee, K. Hooman, Experimental study of fluid flow behaviour and pressure drop in channels partially filled with metal foams, Exp. Therm. Fluid. Sci., 99 (2018) 117–128. https://doi.org/10.1016/j.expthermflusci.2018.07.032

[19] T. Chen, G. Shu, H. Tian, T. Zhao, H. Zhang, Z. Zhang, Performance evaluation of metal-foam baffle exhaust heat exchanger for waste heat recovery, Appl. Energy., 266 (2020). https://doi.org/10.1016/j.apenergy.2020.114875

[20] M.H. Mohammadi, H.R. Abbasi, A. Yavarinasab, H. Pourrahmani, Thermal optimization of shell and tube heat exchanger using porous baffles, Appl. Therm. Eng., 170 (2020) 115005. https://doi.org/10.1016/j.applthermaleng.2020.115005

[21] N.M. Jasim, E.M. Fayyadh, M.R. Hasan, Numerical Study on the Effect of Geometrical Parameter on the Thermal-Hydraulic Performance of the Metal Foam Heat Exchanger, IOP Conf. Ser. Mater. Sci. Eng., 1094 (2021) 012112. https://doi.org/10.1088/1757-899x/1094/1/012112

[22] H.W. Coleman, W.G. Steele, Experimentation, Validation, and Uncertainty Analysis for Engineers, FOURTH, Wiley, New York, 2018. https://doi.org/10.1002/9781119417989

[23] H.Y.Jeong, K. Ha, Y.Kwon, W.P.Chang, & Y. Lee, A correlation for single phase turbulent mixing in square rod arrays under highly turbulent conditions , Nucl. Eng. Technol., 38 (2006) 809-818.

[24] F.W. Dittus, L.M.K. Boelter, Heat Transfer to Water in Thin Rectangular Channels, J. Heat. Transfer., 12 (1985) 3–22.